Silicon Quantum Computer

Kohei M. Itoh
Keio University, Yokohama, Japan

Collaborators: Yoshi Yamamoto and Yoshi Matsumoto

Quantum Information in Group IV Semiconductors Workshop
March 28-29, 2003

Semiconductor Isotope Engineering

List of stable isotopes

^{28}Si 92.2%
^{29}Si 4.7% → 1/2 (nuclear spin)
^{30}Si 3.1%

^{70}Ge 20.5%
^{72}Ge 27.4%
^{73}Ge 7.8% → 9/2 (nuclear spin)
^{74}Ge 36.5%
^{76}Ge 7.8%

^{69}Ga 60.1% → 3/2
^{71}Ga 39.9% → 3/2 (nuclear spin)

^{75}As 100% → 3/2

Mass and nuclear spin control through manipulation of stable isotopes

99.999% ^{28}Si possible with $10k/gram

Isotope effect on thermal conductivity

Thermal conductivity of 99.86% ^{28}Si

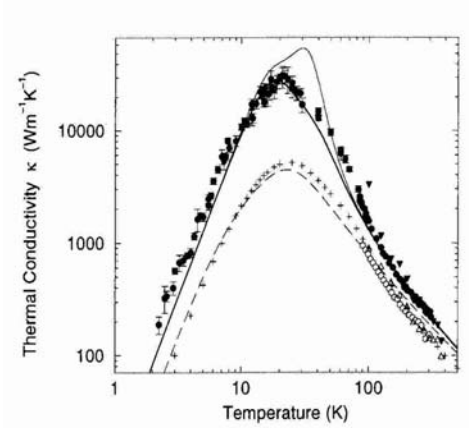

T. Ruf, *et al.* Solid State Commun. 2000

300K 60% increase

400K 40-50% increase

with respect to natural Si

ISONICS, Golden, CO

- 99.92% ^{28}Si epi-layers of 1-100 microns on 4-6 inch Si

^{29}Si nuclear spin quantum computer

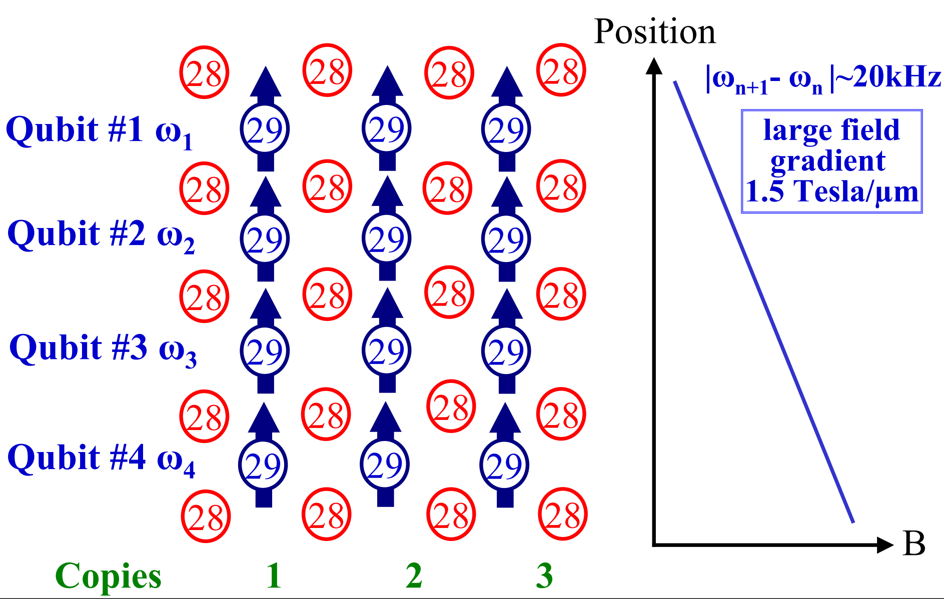

^{29}Si wire fabrication

- Form regular step arrays on slightly miscut ^{28}Si(111)7×7 surface (~ 1° from normal)
- Steps are *straight*, with about 1 kink in 20000 sites.
- ^{29}Si chains formed by "Step Decoration" from ^{28}Si steps
- Angle of miscut controls chain spacing

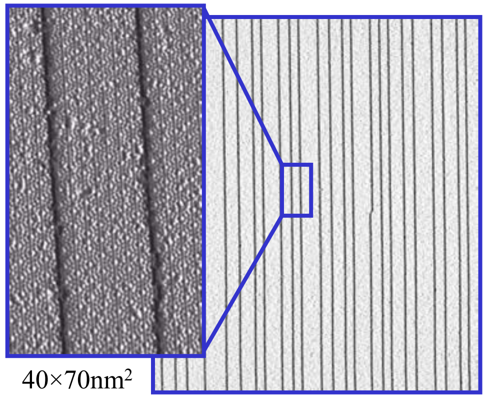

40×70nm²

340×390nm²

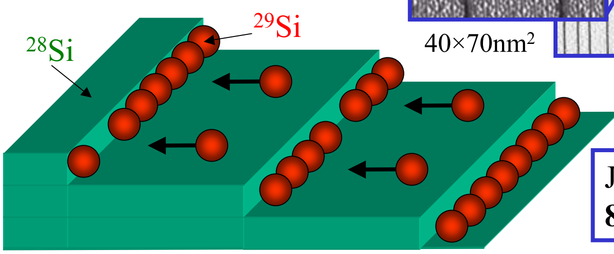

J.-L. Lin, *et al.*, *JAP* **84**, 255 (1998)

Row-by-row growth

The step-flow growth was observed as the appearance of new adatoms at the edge

Short rows are thermally diffused to form a longer row which is energetically stable

T_{sub} 350℃
Growth rate 0.8 × 10^{-2}BL/min

T. Hasegawa, et al., Phys. Rev. B48, 1943 (1995).

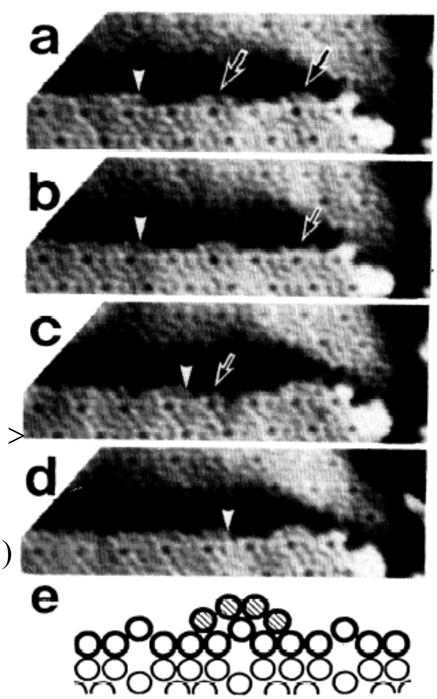

< $\bar{1}\bar{1}2$ >

U(5)

Short-term goal

Homogeneous and strong gradient

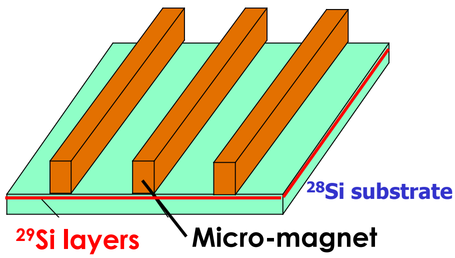

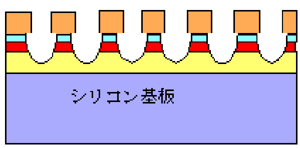

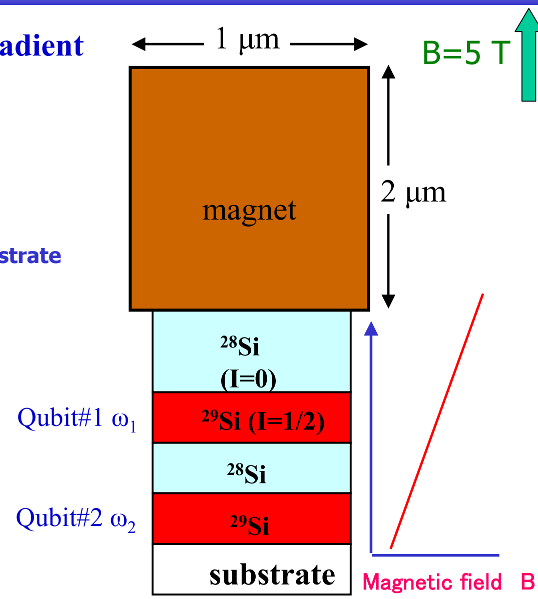

Magnetic field simulation

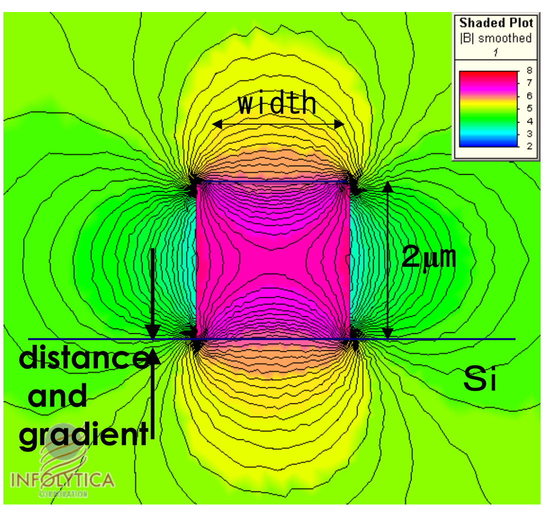

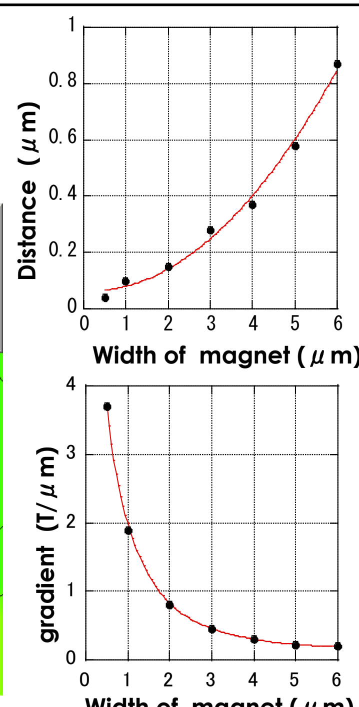

Enriched Si crystals

Natural abundance

^{28}Si: 92.2 %

^{29}Si: 4.7 %

^{30}Si: 3.1 %

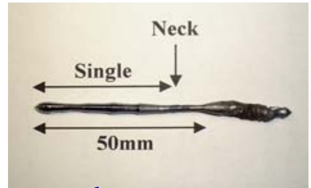

99.92% ^{28}Si single crystal

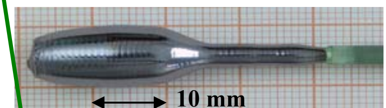

99.3% ^{29}Si single crystal

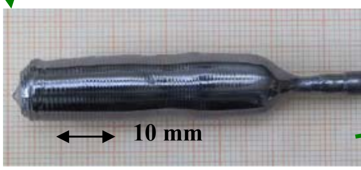

99.3% ^{30}Si single crystal

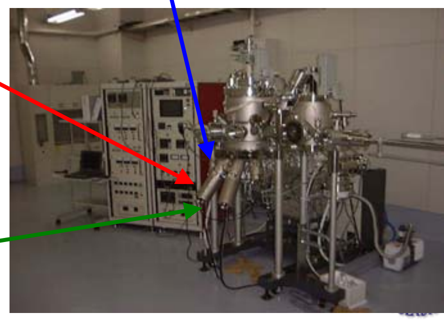

$^{28}Si_n/^{30}Si_n$ Isotope Superlattices

n: # of monolayers

n = 8, 12, 24

1 monolayer = 1.36 Å

^{28}Si layer ≡ $^{nat.}$Si (92.2 % ^{28}Si)

^{30}Si layer ≡ 98.74 % ^{30}Si

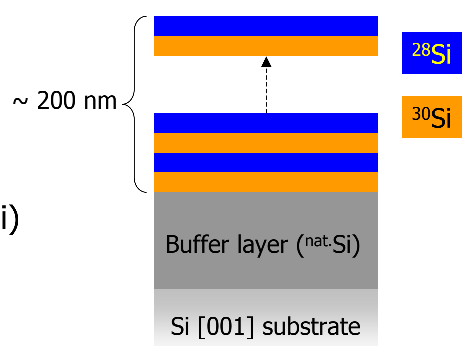

Characterization

Secondary Ion Mass Spectrometry (SIMS)

Raman Spectroscopy

MBE Equipment

Growth conditions

Pressure

~ 5 × 10^{-9} Torr

Temperature

Substrate: 650ºC

K-cells: 1400ºC

Growth rate

0.1 ~ 0.5 Å/sec.

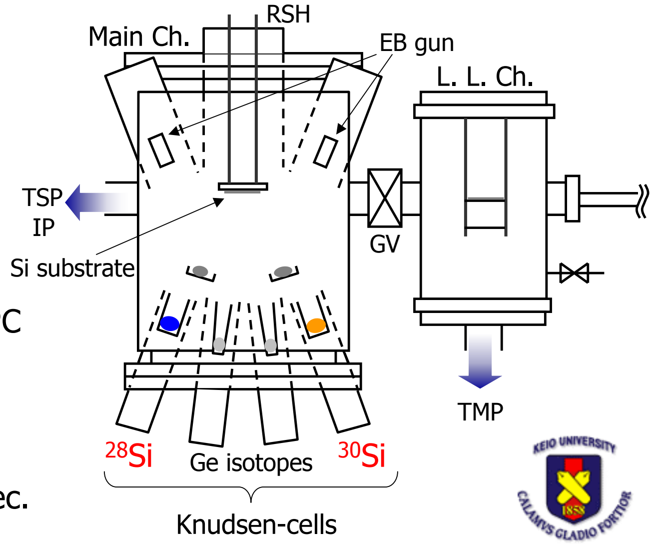

SIMS of Superlattices

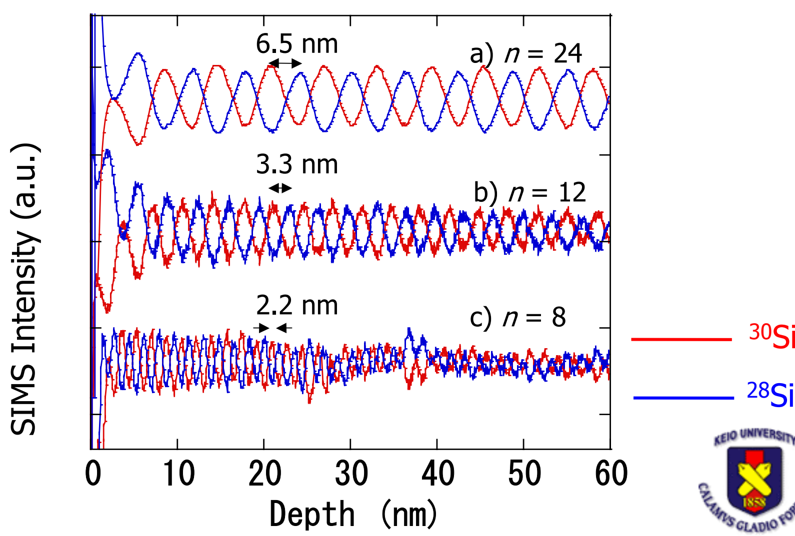

Phonons of Superlattices

Ex) $^{nat.}Si_4/^{30}Si_4$ superlattice

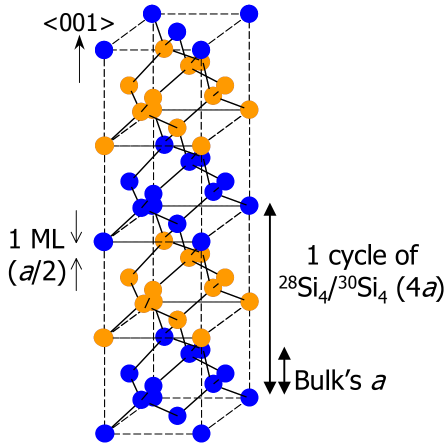

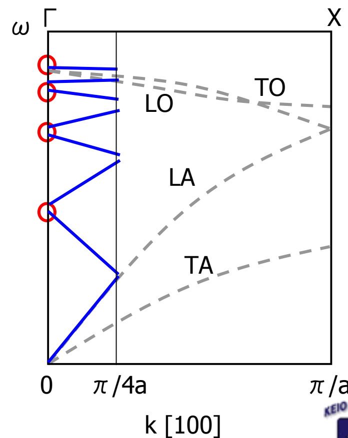

Vibrational modes in $^{28}Si_{12}/^{30}Si_{12}$

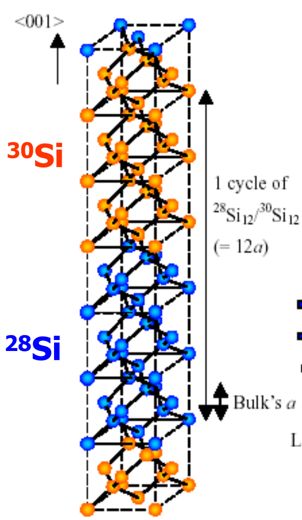

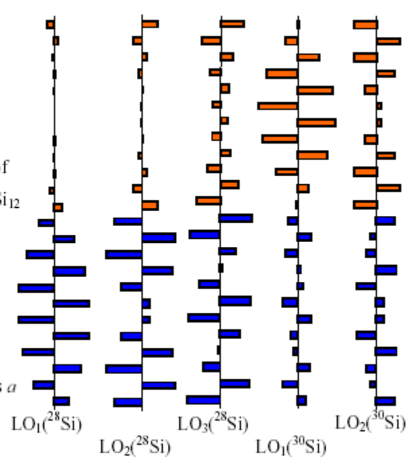

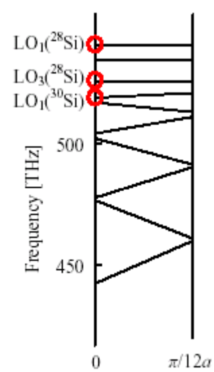

Raman Spectroscopy

Backscattering geometry

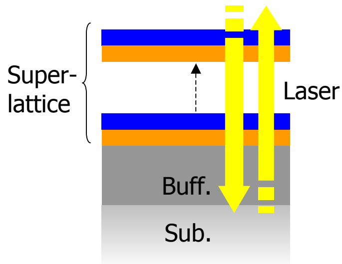

Conditions

✓ Ar^{+} laser (514.5 nm)

✓ ~ 4 K (liq. He)

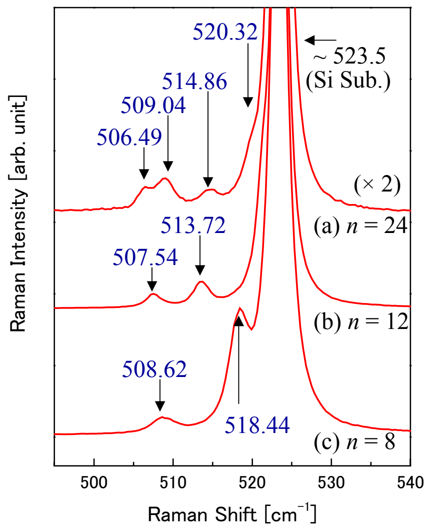

Comparison with theory

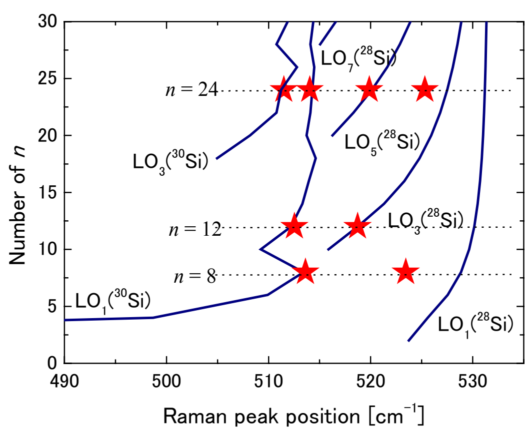

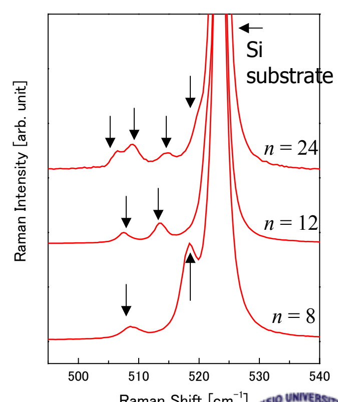

Sputter growth growth and reactive ion etching of NiFe

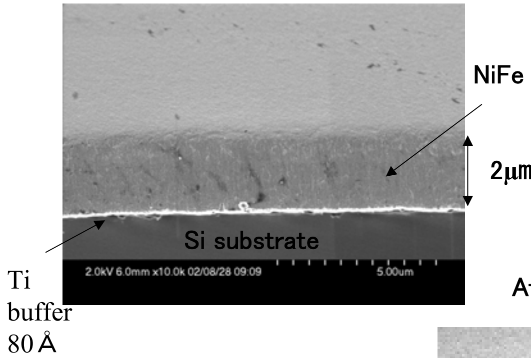

After reactive ion etching

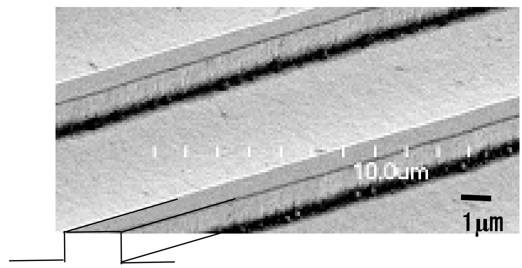

Conclusion

$^{28}Si/^{30}Si$ Isotope Superlattices

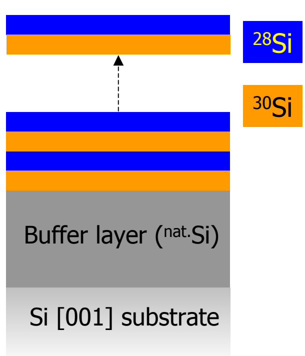

Self-Assembled
Ge/Si(100)Quantum Dots

A. V. Kolobov *et al.*,
APL **81**, 3855 (2002)